Journal of Mining and Environment (JME) Vol. 12, No. 4, 2021, 1077-1088

Shahrood University of Technology

Iranian Society of Mining Engineering (IRSME)

Journal of Mining and Environment (JME)

journal homepage: www.jme.shahroodut.ac.ir

THOMSON REUTERS

Recognition of Gold Mineralization Potentials Based on Rock Samples Utilizing Staged Factor and Fractal Models, Bardaskan District (NE Iran)

Lili Daneshvar Saein*

Department of Geology, Payame Noor University, Tehran, Iran

Article Info

Received 31 August 2021

Received in Revised form 1 November 2021

Accepted 16 November 2021

Published online 16 November 2021

DOI:10.22044/jme.2021.11156.2096

Keywords

Gold mineralization

Concentration–number fractal model

Staged factor analysis

Rock samples

Bardaskan

Abstract

The purpose for this research is to define the gold mineralization potentials by the concentration-number fractal and staged factor analysis modeling based on rock samples at the Bardaskan area (NE Iran). Two main gold mineralization types are epithermal and disseminated systems in this district. First, the staged factor analysis is carried out at four stages. The stepwise factor analysis was applied in three stages to remove noise elements. Moreover, staged factor analysis was applied in the fourth step based on metallic elements including Au, Ag, Cu, As, Fe, Mo, Bi, La, S, Zn, and Cd were grouped. These elements are grouped at four factors, and related factors for gold mineralization are F1-4 (first factor in the fourth stage) which is consisting of As, Mo, S and Fe and F3-4 (third factor in the fourth stage) includes Au and Ag. The concentration-number log–log plots for factor scores of F1-4 and F3-4 were generated, and their threshold values were calculated to create the factor score's geochemical maps. Based on these results, the gold mineralization potentials are positioned in the NE, northern and SE sections of the district, which indicate a correlation among alteration zones, including chloritization, sericitization, and silicification alteration zones and faults and fault's intersections. Main Au mineralization occurred in silicified-sulfidic veins/veinlets in NE and northern portions of the region. However, high grade F3-4 anomalies are located in intersection of faults and neighboring fault zones especially at the northern part of this district. Moreover, Samples with Au≥ 100 ppb were situated in major anomalous parts of F3-4 (Au-Ag) and marginal parts of the F1-4, which include pathfinder of gold mineralization.

1. Introduction

Geochemical exploration modeling is a greatly complex decision-making operation. Two key risk factors, the quality of geochemical data and robustness of the underlying conceptual targeting model, have a strong impact on the effectiveness of this decision-making for generation of mineral prospectivity mapping (MPM) [1-2]. Rock samples are widely used for geochemical exploration of different types of ore deposits. Lithogeochemical anomalies are essential for the further exploration and design of grid drilling. It is essential for the detection of mineralization potentials [3-7]. Many methods were utilized for the recognition of anomalous geochemical areas such as classical statistical analysis and nonlinear techniques [8-10]. Variation of methodology is wide from statistical parameters (e.g., mean and standard deviation) to fractal models, such as concentration-area, concentration-number and fractal-wavelet [11-15].

Multivariate analysis is widely utilized for geochemical exploration for defining paragenesis of ore elements. Stepwise and staged factor analysis can be utilized to find optimum paragenesis proposed by Yousefi et al. (2012) [16] and Yousefi et al. (2014) [17], respectively. This methodology is an advanced technique for multivariate analysis. However, fractal analysis is applied for the categorization of geochemical zones and anomalies [16-19]. Multivariate analysis with fractal modeling was used for the delineation

Corresponding author: daneshvar.saein@gmail.com (L. Daneshvar Saein).

of ore elemental potentials based on better interpretation of geochemical data [22-24].

This paper aims to model geochemical anomalies related to gold mineralization by the staged factor analysis and concentration-area fractal method in the Bardaskan area, NE Iran, based on rock samples.

2. Geological setting

Bardaskan district has an area of about 7.5 km^2, which is located approximately 16 km north of Bardaskan city (NE Iran). This region is positioned at the Taknar zone that is one of the subdivisions of the Iranian central structural zone in the north Darouneh fault [25-26]. Metallic mineralization, specifically gold consist of epithermal and disseminated types [27]. The studied district is mostly included Ordovician metamorphic, volcanoplutonic, and volcanoclastics units from Taknar zone. Volcanoplutonic units are rhyodacite, rhyolite, spillite, and diabase. Besides, the metamorphic lithological units are schist, meta-sandstone especially sericite schist, chlorite schist and slates. Furthermore, schists and tuffaceous sandstones are extended in the district [27].

The major faults have two E-W and NE-SW trends, and feather-type joints and fractures are strong in several parts of this area, as depicted in Figure 1. Major alteration zones include chloritization, sericitization, and silicification types. Major ore minerals include chalcopyrite, pyrite, and gold particles within silicic veins and sericite alteration zones [26-27].

There are several gold mineralization and deposits such as Sebandoon, Bijvard and Damanghor as epithermal gold ores in the north of Bardaskan region [28-30]. The study gold ore is located in Khorasan Razavi and in the central domain on the volcano plutonic belt of north of Daruneh fault and Taknar zone. Some of the units of upper and lower parts of Taknar formation in this area have outcrop. The igneous rocks of this area involved rhyolite and rhyodacite are related to the lower part of Taknar formation and volcanoclastic rocks involved tuffaceous sandstones and also metamorphic rocks of this area involved shist and filit are related to upper part of Taknar formation. The mineralization in this area has been seen in two forms of veines/veinlets and disseminated. The mineralization in form of vein has been occurred in the fractures and faults and has seen in form of the veins of quartz and quartz-sulfide that in the quartz-sulfide veins, sulfide frequently is chalcopyrite and occasionally pyrite. The mineralization in form of dispersed also has seen in form of distributed inside the altered host rocks (the metamorphic tuffaceous sandstones and shists) of this area. Based on the studies of the fluid inclusions, isotopic and other witnesses discussed in this paper, could introduce the gold deposit of Bardaskan area similar to the epithermal low sulfidization type gold deposits such as mentioned gold deposits in this region.

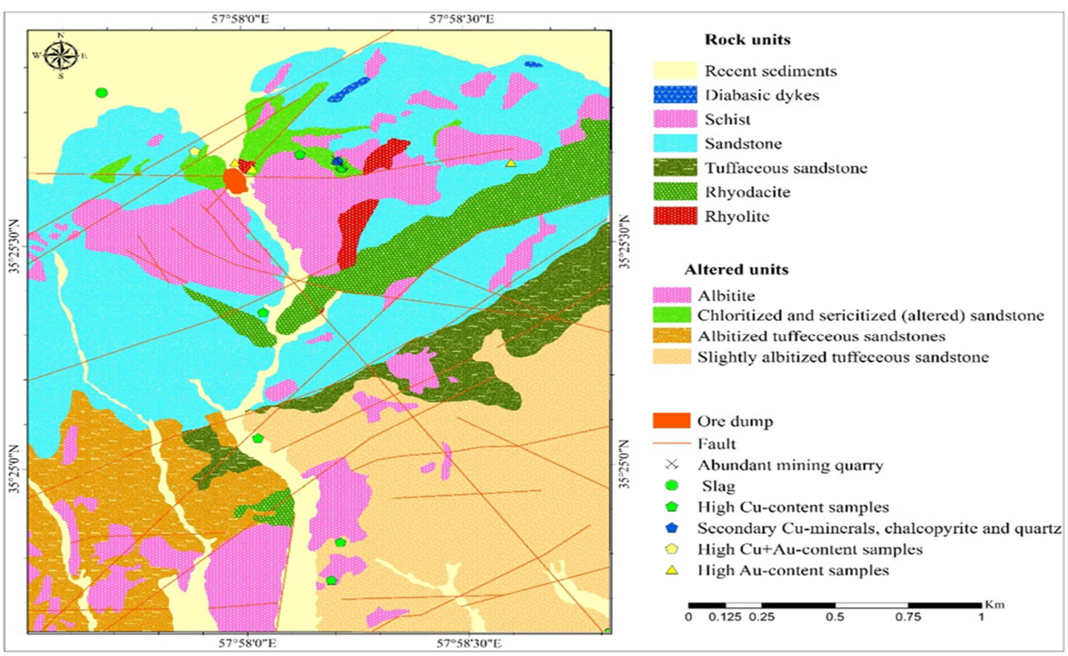

Figure 1. Location of Bardaskan area in Iranian structural map (Alavi, 1994) and Geological map of the area (Hashemi and Afzal, 2013).

3. Methodology
3.1. Staged factor analysis

The multivariate numerical analysis, specifically staged factor analysis, is an appropriate method. This methodology is used to categorize and decrease the number of geochemical variables and finding paragenesis of ore elements. This analysis is an applied instrument to combine several correlated variables (elements in this study) into a single variable and based on correlations of variables or covariance [31-32]. On the other hand, a large dataset of elements are hybrid into a few groups (factors) [16, 17, 33, 34]. The staged factor analysis is an advanced multivariate method to remove noise elements and defining elemental paragenesis for a different scale of mineral exploration [13, 17]. After removing noise elements, target factors are separated and regrouped. It is used for gold and related elements factors in this paper based on rock samples.

Multivariate approaches are used to decrease the dimensionality, so that the procedure and variability of the dataset can be better interpreted by reduced data. The principal component analysis is an orthogonal linear transformation that transmits the data to the original coordinate system. The first component among the principal components which is indicated by y1, is generated as a linear combination of the initial variables x1 to xp:

$Y1 = a11x1+ a12x2 + a13x3 + \ldots + a1_p\, x_p$

The above equation can be characterized in the following form of matrix:

$Y1 = [a1]^T [x]$

There is most variance and variability along the axis. Meanwhile, the different values are the similar to diffraction of the principal components. For the evaluation of the first variable, the first component or the y1 variable is estimated as following form:

$S_{2y1} = [a_1]^T [S][a_1]$

The [S] is the covariance matrix with the principal variables [16]. Following the first component, the second component has the most variability, and these two components are non-correlated. This number of principal components are based on the number of original correlated variables. The staged factor analysis is a developed form of the factor analysis [17].

3.2. Concentration-Number Fractal

Fractal methodology has a commonly applied tool in various branches of geology and mining engineering. This methodology was proposed by Mandelbrot (1983) [35] as a fundamental method entitled number-size (N-S). Consequently, the concentration–number (C-N) fractal model is improved based on N-S method by Sadeghi et al. (2012) [18] as follows:

$$N(\geq C) \propto C^{-\alpha} \quad (1)$$

N(≥C) is the number of the studied regionalized variable greater than the α value, and α is a fractal dimension. These data are modeled as raw data without any estimation or simulation [3, 22]. C-N log-log plot denotes grade distribution and the relationship between anomalous areas [4]. Thus, there is an association among different ore grades and their sample cumulative number based on the ore grades at a case study [32].

4. Discussion
4.1. Dataset

There are 483 collected rock samples in a symmetrical grid (Figure 2). ICP-MS analyzed them for elements that relate to gold mineralization. Statistical parameters for gold are equal to 38 ppb, 18 ppb, and 8 ppm for mean, median, and maximum values, respectively. Statistical characteristics for gold and related elements were shown in Table 1. The gold distribution is not normal and has a wide range's variation between maximum and minimum (Figure 3).

Table 1 Statistical parameters of Au, Cu, As, and Sb in the Bardaskan area

Element	Au (ppb)	Cu (ppm)	As (ppm)	Sb (ppm)
Mean	38	437	10.3	1.72
Median	18	41	21	7
Standard Deviation	357	3000	28.3	1.83
Maximum	8,540	46,730	1,060	39
Minimum	1	1	5	5

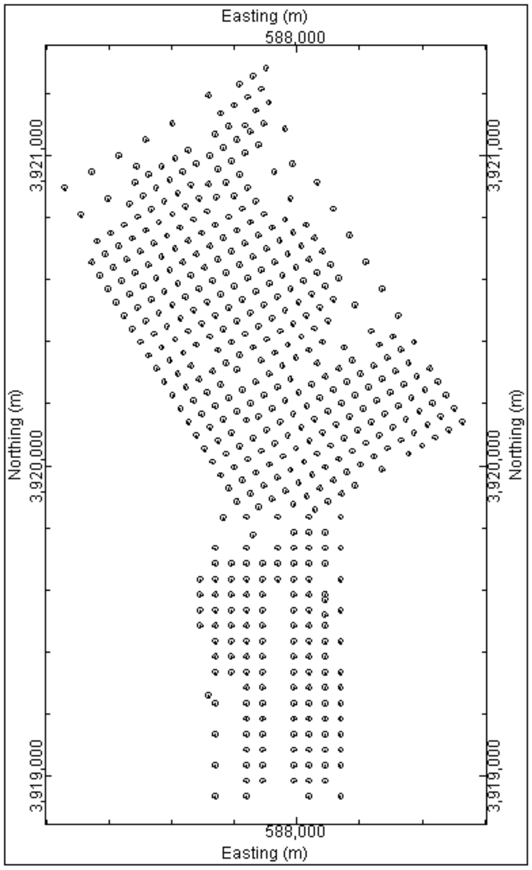

Figure 2. Rock sampling grid in the Bardaskan area

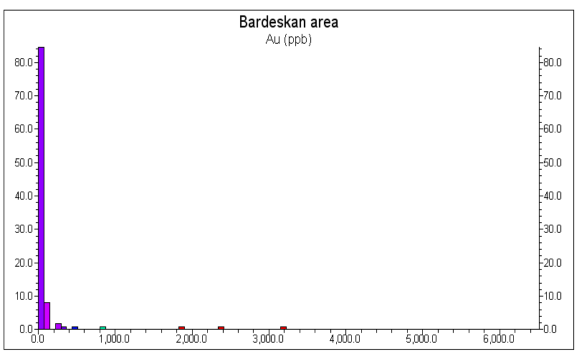

Figure 3. Gold histogram in the Bardaskan district

4.2. Results

These rock samples' data were transformed by an Ln transformation for the staged factor analysis. For decreasing variables' number, staged factor analysis was achieved in different geochemical data. The staged factor analysis was used for 34 elements of bardaskan area, which were classified by applying SPSS software to the related groups; for an improved representation of the extracted factors, the factor plot at rotated space is indicated in Figure 4. The stepwise factor analysis was used to the three steps of rock samples data for removing noisy elements (Table 2). These elements were removed from the dataset, and factors were cleaned for staged factor analysis in the fourth stage. Hence, scores for the noisy elements are lower than 0.5. The threshold value of 0.5 was utilized for loading at the staged factor analysis to identify highly contributing elements in the factors, according to the rotated matrix [13]. Based on the stepwise factor analysis, noisy elements were removed, as depicted in table 1. Finally, 11 elements include Au, As, Ag, Cu, Mo, Zn, Fe, S, Bi, La, and Cd were selected for the final step for staged factor analysis based on gold mineralization (Tables 3; Figure 4). Finally, Au and As (main pathfinder element for gold mineralization) were grouped in the first and third factors in the fourth stage (F1-4 and F3-4). The gold is grouped with silver in F3-4 and As with Mo, Fe and S had existed in the F1-4.

Based on C-N log-log plots of these factors, four geochemical populations of F1-4 and F3-4 are existed, as depicted in Figure 5. Main populations start from 0.63 and 0.35 for F1-4 and F3-4, respectively. Furthermore, extremely anomalous parts commence from 2.51 and 3.16 for F1-4 and F3-4, respectively.

5. Discussion

Major anomalies of these factors are positioned in the eastern and NE parts of this region to each other, and small parts for F3-4 at the central and SE portions of the Bardaskan district (Figure 6). For validation, collected further samples from the trenches of detailed exploration were used. Samples with Au≥ 100 ppb were situated in major anomalous parts of F3-4 (Au-Ag) and marginal parts of the F1-4, which include pathfinder of gold mineralization, as shown in Figure 6. Alteration zones have an appropriate relationship with these factors' anomalies. Major anomalies of these factors are associated with chloritization, sericitization, and silicification alteration zones. The chloritization alteration zone is associated with Cu anomalies, as shown in Figure 7. Main alteration zones are silicification in the northern part of this area which is correlated with main anomalies. Sericitizations are existed in several parts of the north of this area (Figure 7). Comparison of the main characteristics of this deposit with epithermal gold deposits reveals that the geology, alteration, mineralography and geochemical characteristics are similar to the epithermal deposits.

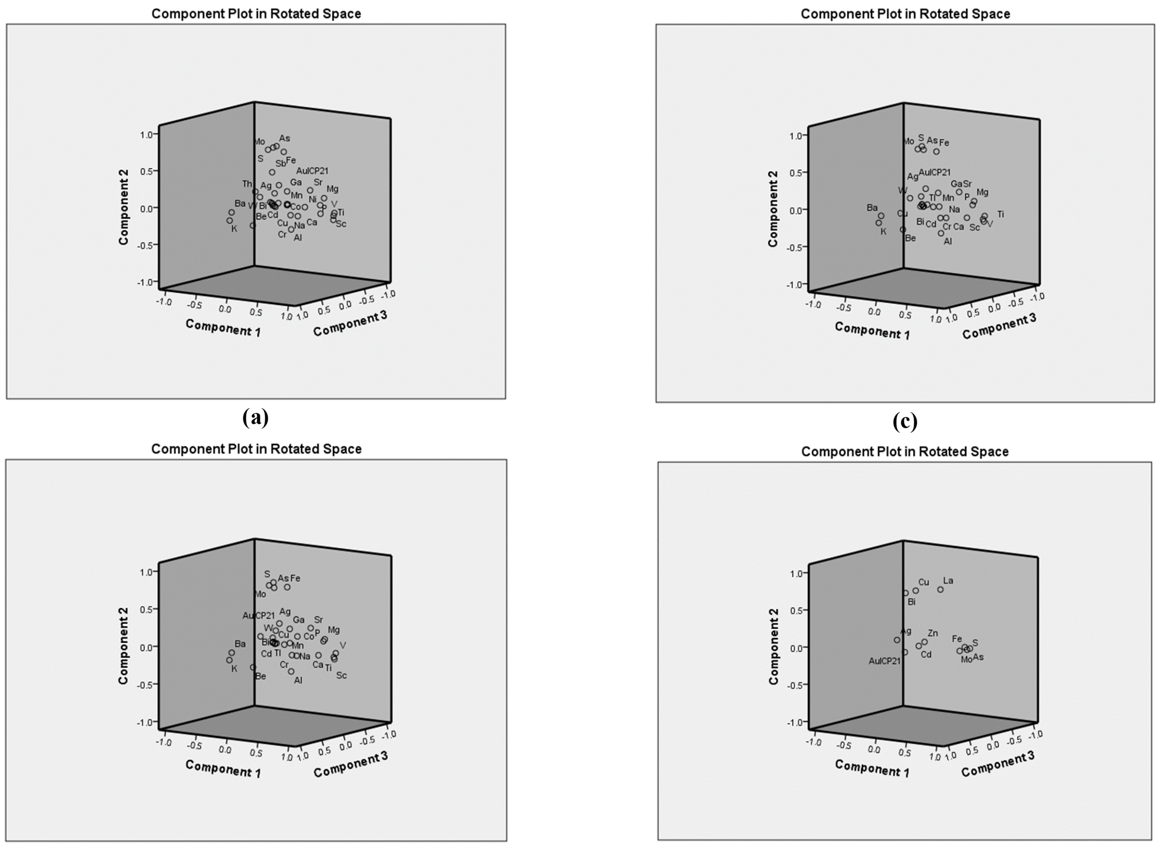

(a) (c)

(b) (d)

Figure 4. Component plots in rotated space in first (a), second (b), third (c) and fourth (d) stages of staged factor analysis

Table 2. The three stages of stepwise factor analysis of Bardaskan rock samples. Bold values indicate existing elements in each factor (Based on absolute threshold of 0.5).

	First stage										
	Component										
	1	2	3	4	5	6	7	8	9	10	11
Ag	-.032	.135	-.041	.040	-.076	**.792**	.138	.007	.056	-.067	.039
Al	.396	-.279	.186	**.721**	.278	-.150	.068	-.007	.019	-.010	-.081
As	-.027	**.770**	-.078	.126	.027	-.049	.152	.098	-.001	-.147	-.097
Ba	-.111	-.003	**.849**	.012	-.090	-.070	.066	.027	.014	-.041	.012
Be	.016	-.213	.535	**.595**	-.108	-.048	.172	-.027	.115	-.003	.025
Bi	-.037	-.025	-.005	-.090	-.104	.498	-.084	.112	**.622**	.044	.021
Ca	**.710**	-.068	-.049	-.302	.009	-.021	.092	-.036	-.045	-.116	.163
Cd	.023	-.018	.042	-.033	.033	.192	**.749**	-.051	-.064	-.013	-.069
Co	.167	.010	-.046	.025	.050	-.096	-.024	.009	.029	**.779**	.061
Cr	.278	-.120	.030	.071	.136	.087	-.089	**.742**	-.054	.106	-.112
Cu	-.099	-.008	-.069	-.085	-.100	.236	.090	.454	**.583**	.161	-.025
Fe	.046	**.690**	-.141	-.124	-.239	.068	-.013	-.046	.017	.290	.299
Ga	.219	.197	.027	**.770**	.007	.205	-.094	-.083	.008	.081	.079
K	-.139	-.115	**.853**	.255	-.251	.030	-.008	.031	.014	-.095	-.023
La	.096	.029	.055	.125	.006	-.116	-.021	-.097	**.770**	-.033	-.033
Mg	.434	.047	**-.526**	.298	-.287	-.084	.193	-.173	.044	-.040	.074
Mn	.157	-.004	-.084	-.178	-.166	-.048	.392	-.157	.044	.265	**.566**
Mo	-.213	**.693**	-.148	-.027	-.148	.160	-.113	.025	-.033	.041	.071
Na	.248	-.166	-.182	.092	**.811**	-.162	-.034	.066	-.010	.006	-.139
Ni	.443	-.008	-.067	.353	.007	-.074	.220	.298	.002	.474	-.115
P	**.701**	.046	-.054	.208	.003	-.009	-.071	-.105	.113	.368	-.020
Pb	-.006	.037	.097	.048	.094	**.608**	.304	.082	-.006	-.010	-.031
S	.005	**.773**	.046	-.137	.054	.183	-.116	-.196	.023	.021	-.088

Table 2. Continues of Table 2

Sb	.099	.470	.204	.171	-.077	-.044	.365	.167	.121	-.187	-.023
Sc	**.880**	-.087	-.111	.233	.005	-.080	.014	.083	.009	.000	.133
Sr	**.697**	.280	.173	-.182	.303	.059	-.087	-.163	.036	.129	-.012
Th	-.234	.160	.119	.074	.449	-.071	-.076	-.222	.375	-.332	.159
Ti	**.867**	-.145	-.123	.180	-.028	-.051	-.011	.041	-.009	.111	.078
Tl	.216	.009	.025	.107	.094	.039	-.056	.120	-.041	-.057	**.773**
U	-.098	-.073	-.154	-.010	**.776**	.023	-.025	.022	-.103	.054	.090
V	**.863**	-.058	-.154	.285	-.057	-.023	.023	.136	-.063	.127	.069
W	-.177	.088	.093	-.121	-.043	-.042	-.091	**.660**	.062	-.072	.171
Zn	-.036	-.002	.000	.048	-.068	.079	**.784**	-.079	.007	.030	.108
Au-ICP21	-.138	.198	-.293	-.002	-.328	**.520**	-.150	-.102	.011	-.130	.009

Extraction Method: Principal Component Analysis.
Rotation Method: Varimax with Kaiser Normalization.[a]
a. Rotation converged in 10 iterations.

Table 2. Continues of Table 2

	Second stage									
	Component									
	1	2	3	4	5	6	7	8	9	10
Ag	-.023	.151	-.049	.040	-.057	.200	**.746**	.176	.036	.083
Al	.398	-.314	.194	**.700**	.279	.046	-.133	-.031	-.046	-.091
As	-.038	**.724**	-.033	.144	.037	.119	.020	-.063	.038	-.110
Ba	-.113	-.022	**.844**	.007	-.113	.063	-.074	-.010	.044	.004
Be	.020	-.248	**.536**	.587	-.104	.145	-.054	.096	-.062	.040
Bi	-.037	.000	-.001	-.064	-.061	-.051	.407	**.719**	.077	.070
Ca	**.691**	-.100	-.020	-.332	.004	.056	.065	-.122	-.062	.140
Cd	.026	-.007	.043	-.028	.020	**.796**	.109	-.045	-.030	-.060
Co	.258	.088	-.151	.022	-.006	.058	-.422	.197	.156	.140
Cr	.291	-.132	.024	.063	.162	-.066	.049	.017	**.738**	-.093
Cu	-.079	-.007	-.071	-.072	-.092	.105	.122	**.645**	.420	.008
Fe	.083	**.725**	-.164	-.095	-.256	.021	-.059	.081	.023	.322
Ga	.256	.213	.025	**.776**	-.005	-.038	.148	.031	-.032	.056
K	-.138	-.121	**.862**	.251	-.257	.008	.043	.003	.047	-.043
La	.083	.013	.082	.149	.008	-.042	-.157	**.697**	-.176	-.076
Mg	.450	.018	**-.509**	.283	-.323	.177	-.042	-.054	-.170	.015
Mn	.169	-.003	-.101	-.177	-.178	.346	-.130	.062	-.158	**.637**
Mo	-.191	**.724**	-.134	-.001	-.158	-.066	.129	-.006	.071	.056
Na	.228	-.176	-.176	.085	**.827**	-.054	-.156	-.028	.011	-.122
P	**.734**	.084	-.074	.200	.023	-.037	-.150	.195	-.085	.035
Pb	.013	.077	.072	.055	.076	.420	.482	.094	.170	-.054
S	.021	**.814**	.067	-.118	.046	-.056	.143	.045	-.156	-.101
Sc	**.883**	-.118	-.102	.222	.002	.007	-.065	-.045	.084	.096
Sr	**.701**	.291	.175	-.196	.308	-.070	.009	.059	-.155	.016
Ti	**.876**	-.148	-.125	.173	-.014	.001	-.085	-.007	.053	.076
Tl	.187	.002	.053	.125	.132	-.101	.081	-.056	.078	**.770**
U	-.108	-.039	-.156	-.001	**.788**	-.007	-.017	-.069	.018	.109
V	**.874**	-.075	-.159	.276	-.033	.023	-.053	-.046	.137	.082
W	-.173	.080	.091	-.098	-.074	-.053	-.063	.034	**.707**	.060
Zn	-.033	.001	.009	.057	-.077	**.797**	.003	.006	-.085	.129
Au-ICP21	-.128	.202	-.283	-.013	-.322	-.130	**.579**	.051	-.088	.018

Extraction Method: Principal Component Analysis.
Rotation Method: Varimax with Kaiser Normalization.[a]
a. Rotation converged in 10 iterations.

Table 2. Continues of Table 2

	Third stage									
	Component									
	1	**2**	**3**	**4**	**5**	**6**	**7**	**8**	**9**	**10**
Ag	-.033	.125	.020	.054	-.002	.201	**.815**	.085	.022	.034
Al	.395	-.305	.169	**.709**	.263	.052	-.186	-.001	-.037	-.084
As	-.040	**.743**	-.045	.146	.038	.147	-.013	-.031	.065	-.109
Ba	-.109	-.024	**.845**	.019	-.118	.064	-.102	-.011	.039	-.001
Be	.018	-.243	.517	**.594**	-.117	.146	-.092	.117	-.054	.048
Bi	-.035	-.008	.034	-.067	-.026	-.035	.491	**.676**	.100	.048
Ca	**.689**	-.093	-.015	-.320	.015	.085	.050	-.119	-.045	.127
Cd	.027	.002	.060	-.019	.041	**.821**	.116	-.046	-.013	-.074
Cr	.295	-.128	.039	.065	.175	-.060	.064	-.010	**.742**	-.106
Cu	-.072	-.001	-.058	-.085	-.077	.109	.190	**.628**	.445	.008
Fe	.091	**.715**	-.158	-.113	-.257	-.010	.027	.062	.004	.335
Ga	.252	.203	.031	**.777**	.003	-.046	.182	.008	-.043	.045
K	-.140	-.120	**.856**	.266	-.262	.012	-.010	.008	.048	-.046
La	.081	.030	.042	.143	-.021	-.049	-.176	**.752**	-.147	-.042
Mg	.446	.029	**-.531**	.275	-.329	.187	-.029	-.027	-.153	.027
Mn	.181	-.007	-.094	-.191	-.170	.343	-.041	.050	-.156	**.640**
Mo	-.191	**.724**	-.127	-.008	-.149	-.067	.156	-.015	.072	.056
Na	.230	-.167	-.187	.089	**.817**	-.048	-.208	-.003	.018	-.117
P	**.737**	.074	-.081	.195	.009	-.073	-.096	.187	-.107	.050
S	.019	**.811**	.077	-.114	.052	-.059	.147	.041	-.161	-.103
Sc	**.882**	-.109	-.116	.226	-.002	.019	-.068	-.031	.097	.099
Sr	**.703**	.283	.186	-.185	.311	-.076	.021	.046	-.166	.009
Ti	**.878**	-.143	-.138	.174	-.022	-.001	-.082	.004	.059	.086
Tl	.178	.009	.041	.133	.130	-.091	.047	-.043	.090	**.773**
U	-.103	-.041	-.144	.000	**.795**	-.004	-.029	-.077	.015	.098
V	**.875**	-.073	-.164	.277	-.033	.027	-.024	-.050	.139	.080
W	-.173	.095	.078	-.101	-.085	-.064	-.098	.049	**.714**	.080
Zn	-.033	.017	.005	.060	-.072	**.816**	-.008	.031	-.060	.133
Au-ICP21	-.133	.183	-.229	-.011	-.268	-.097	**.669**	-.021	-.083	-.030

Extraction Method: Principal Component Analysis.
Rotation Method: Varimax with Kaiser Normalization.[a]

a. Rotation converged in 9 iterations.

Table 3. The final stage of staged factor analysis of Bardaskan rock samples. Bold values indicate existing elements in each factor (Based on absolute threshold of 0.5).

	Rotated Component Matrix[a]			
	Component			
	1	2	3	4
Ag	.102	.168	**.765**	.231
As	**.745**	.003	-.033	.115
Bi	.001	**.739**	.420	-.053
Cu	.000	**.737**	.180	.029
Fe	**.760**	.043	.110	-.016
La	.057	**.686**	-.320	.012
Mo	**.759**	.009	.230	-.070
S	**.784**	.009	.093	-.031
Zn	.024	.025	.007	**.840**
Au-ICP21	.220	.013	**.751**	-.087
Cd	-.023	-.025	.077	**.852**

Extraction Method: Principal Component Analysis.
Rotation Method: Varimax with Kaiser Normalization.[a]

a. Rotation converged in 5 iterations.

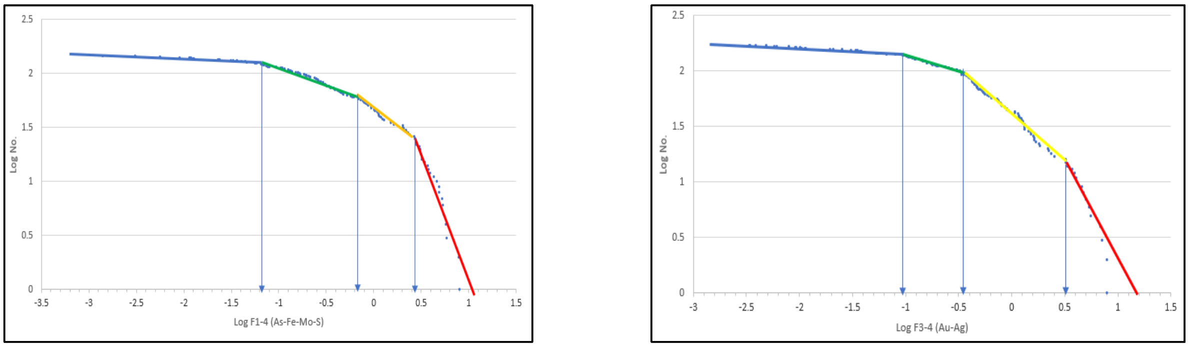

Figure 5. C-N log-log plots for F1-4 and F3-4

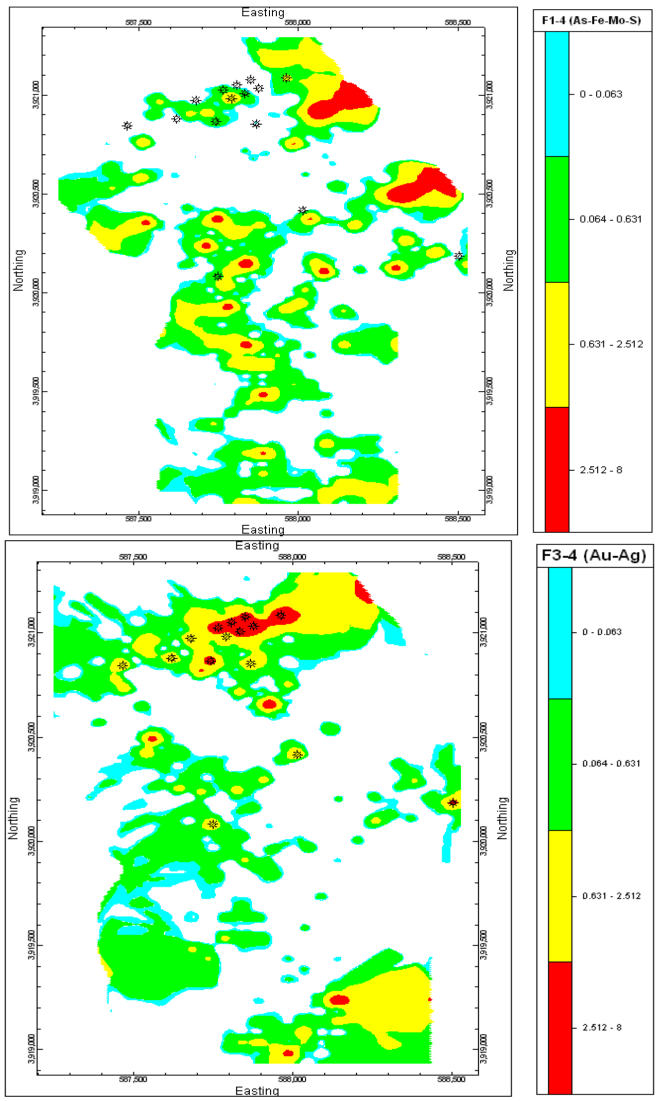

Figure 6. Correlation between geochemical maps of F1-4 and F3-4 in the Bardaskan area with further rock samples (black stars are further samples)

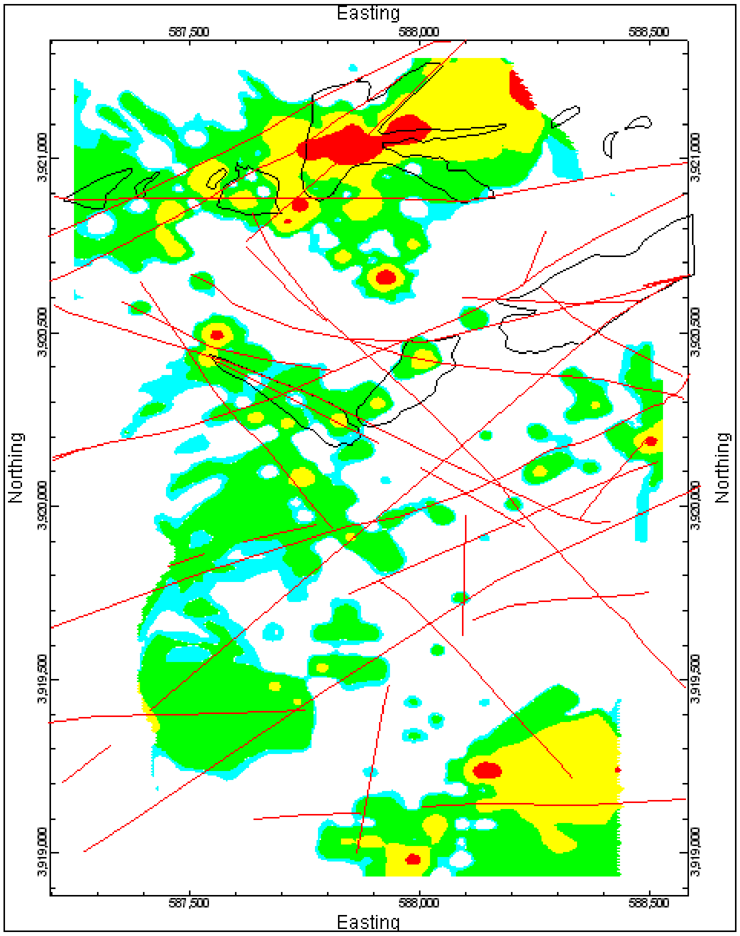

Figure.7. Correlation between geochemical map of F3-4 in the Bardaskan area with alteration zones (polygons) and faults (red lines)

6. Conclusion

The multivariate fractal modeling was achieved to recognize anomalies of related factors for gold mineralization in the Bardaskan district, NE Iran. These anomalies have a proper correlation with different alteration zones and faults, especially faults' intersections. Besides, this multivariate fractal analysis can be a valuable technique for the exploration of mineralization potentials. The this methodology advantages basically rely on its accuracy based on removing noises from geochemical data and better separation of factors related to target mineralization. Main mineralization potentials for gold are situated in the NE, eastern and central parts of this area. These potentials were validated for faults, alteration zones, and further collected samples from trenches. These results show that this hybrid method is appropriate for geochemical exploration based on rock samples. Major Au mineralization happened in silicified and sulfidic veins/veinlets at the northern part of this region. However, high-intensity F3-4 anomalies are located at near fault and fault intersections zones specifically in the north of the Bardaskan area. In addition, Samples with Au≥ 100 ppb were situated in major anomalous parts of F3-4 (Au-Ag) and marginal parts of the F1-4, which include pathfinder of gold mineralization.

References

[1]. Yousefi, M., Carranza, E.J.M., Kreuzer, O.P., Nykänen, V., Hronsky, J.M.A. (2021). Data analysis methods for prospectivity modelling as applied to mineral exploration targeting: State-of-the-art and outlook. Journal of Geochemical Exploration 229, 106839.

[2]. Yousefi, M., Kreuzer, O.P., Nykänen, V., Hronsky, J.M.A. (2019). Exploration information systems – A proposal for the future use of GIS in mineral exploration targeting. Ore Geology Reviews 111, 103005.

[3]. Daneshvar Saein, L., Rasa, I., Rashidnejad Omran, N., Moarefvand, P., Afzal, P. (2014). Application of number-size (N-S) fractal model to quantify of the

vertical distributions of Cu and Mo in Nowchun porphyry deposit (Kerman, SE Iran), Archives of Mining Sciences. 58 (1): 89–105.

[4]. Afzal, P., Yasrebi, A.B., Daneshvar Saein, L., Panahi, S. (2017). Prospecting of Ni mineralization based on geochemical exploration in Iran. Journal of Geochemical Exploration 181, 294-304.

[5]. Nazarpour, A., 2018. Application of C-A fractal model and exploratory data analysis (EDA) to delineate geochemical anomalies in the: Takab 1:25,000 geochemical sheet, NW Iran. Journal of Earth Sciences, 10, 173-180.

[6]. Pourgholam, M.M., Afzal, P., Yasrebi, A.B., Gholinejad, M., Wetherelt, A. (2021). Detection of geochemical anomalies using a fractal-wavelet model in Ipack area, Central Iran. Journal of Geochemical Exploration 220, 106675.

[7]. Shahbazi, S., Ghaderi, M., Afzal, P. (2021). Prognosis of gold mineralization phases by multifractal modeling in the Zehabad epithermal deposit, NW Iran. Iranian Journal of Earth Sciences 13, 31-40.

[8]. Davis, J.C. (2002). Statistics and data analysis in Geology (3th ed.), John Wiley & Sons Inc., New York, p. 342-353.

[9]. Afzal, P., Mirzaei, M., Yousefi, M., Adib, A., Khalajmasoumi, M., Zia Zarifi, A., Foster, P., Yasrebi, A.B. (2016). Delineation of geochemical anomalies based on stream sediment data utilizing fractal modeling and staged factor analysis. Journal of African Earth Sciences 119, 139-149.

[10]. Zuo, R., Agterberg, F.P., Cheng, Q., Yao, L. (2009). Fractal characterization of the spatial distribution of geological point processes. International Journal of Applied Earth Observation and Geoinformation. 11 (6): 394-402.

[11]. Daneshvar-Saein, L. (2017). Delineation of enriched zones of Mo, Cu and Re by concentration-volume fractal model in Nowchun Mo-Cu porphyry deposit, SE Iran. Iran Journl Earth Sciences, 9, 64-72.

[12]. Jebeli, M., Afzal, P., Pourkermani, M., Jafarirad, A.R. (2018). Correlation between rock types and copper mineralization using fractal modeling in Kushk-e-Bahram deposit, Central Iran. Geopersia Journal 8 (1), 131-141.

[13]. Saadati, H., Afzal, P., Torshian, H., Solgi, A. (2020). Geochemical exploration for Li using Geochemical Mapping Prospectivity Index (GMPI), fractal and Stage Factor Analysis (SFA) in NE Iran. Geochemistry: Exploration, Environment, Analysis 20, 461-472.

[14]. Malaekeh, A., Ghasemi, M.R., Afzal, P., Solgi, A. (2021). Fractal modeling and relationship between thrust faults and carbonate-hosted Pb-Zn mineralization in Alborz Mountains, Northern Iran. Geochemistry, 125803.

[15] Shamseddin Meigooni, M., Lotfi, M., Afzal, P., Nezafati, N., Kargar Razi, M. (2021). Application of multivariate geostatistical simulation and fractal analysis for detection of rare earth elements (REEs) geochemical anomalies in Esfordi phosphate mine, Central Iran. Geochemistry: Exploration, Environment, Analysis21, geochem2020-035, 1-17, https://doi.org/10.1144/geochem2020-035.

[16]. Yousefi M., Kamkar-Rouhani A., Carranza, E.J.M. (2012). Geochemical mineralization probability index (GMPI): a new approach to generate enhanced stream sediment geochemical evidential map for increasing probability of success in mineral potential mapping. Journal of Geochemical Exploration, 115, 24-35.

[17]. Yousefi, M., Kamkar-Rouhani, A., Carranza, E.J.M. (2014). Application of staged factor analysis and logistic function to create a fuzzy stream sediment geochemical evidence layer for mineral prospectivity mapping. Geochemistry: Exploration, Environment, Analysis. 14 (1): 45-58.

[18]. Sadeghi, B., Moarefvand, P., Afzal, P., Yasrebi, A.B., Saein, L.D. (2012). Application of fractal models to outline mineralized zones in the Zaghia iron ore deposit, Central Iran. Journal of Geochemical Exploration, 122, 9–19.

[19]. Sadeghi, B., Yilmaz, H., Pirajno, F. (2021). Weighting of BLEG data with drainage and catchment properties to enhance Au anomalies, Geochemistry. 81 (2): 125733.

[20]. Chen, G., Cheng, Q. (2018). Fractal-Based Wavelet Filter for Separating Geophysical or Geochemical Anomalies from Background. Mathematical Geosciences 50, 249-272.

[21]. Aliyari, F., Afzal, P., Lotfi, M., Shokri, S., Feizi, H. (2020). Delineation of geochemical haloes using the developed zonality index using multivariate and fractal analysis in the Cu-Mo porphyry deposits. Applied Geochemistry, 121, 104694.

[22]. Afzal, P., Yousefi, M., Mirzaei, M., Ghadiri-Sufi, E., Ghasemzadeh, S., Daneshvar Saein, L. (2019). Delineation of podiform-type chromite mineralization using Geochemical Mineralization Prospectivity Index (GMPI) and staged factor analysis in Balvard area (southern Iran). Journal of Mining and Environment 10: 705-715.

[23]. Kouhestani, H., Ghaderi, M., Afzal, P., Zaw, K. (2020). Classification of pyrite types using fractal and stepwise factor analyses in the Chah Zard gold-silver epithermal deposit, central Iran. Geochemistry: Exploration, Environment, Analysis 20, 496-508.

[24]. Torshizian, H., Afzal, P., Rahbar, K., Yasrebi, A.B., Wetherelt, A., Fyzollahhi, N. (2021). Application of modified wavelet and fractal modeling for detection of geochemical anomaly. Geochemistry, 125800.

[25]. Alavi, M. (1994). Tectonics of Zagros Orogenic belt of Iran, new data and interpretation. Tectonophysics 229, 211 –238.

[26]. Hashemi, M., Afzal, P., Rasa, I., Noghreian, M., Khosro Tehrani, Kh., Vosoughi Abedini, M. (2010). Geochemical anomaly separation by concentration-area fractal model in Bardaskan area, NE Iran. Journal of Mining and Metallurgy. 46 A (1): 1–10.

[27]. Hashemi, M., Afzal, P. (2013). Identification of geochemical anomalies by using of number-size (N-S) fractal model in Bardaskan area, NE Iran. Arabian Journal of Geosciences 6, 4785–4794.

[28]. Hamami Pour, B., Tajeddin, H.A., Barahmand, L. (2014). Geology and geochemistry of Sebandoon gold mine,north of Bardaskan: Example of epithermal gold mineralization in Ophiolitic host rocks. Conference: 18th Symposium of the Geological Society of Iran (In Persian with Enlish abstract).

[29]. Miri, H., Karimpour, M.H., Malekzadeh Shafaroudi, A. (2020). Geology, mineralization and geochemistry of Bijvard epithermal gold prospect area, Northern Bardaskan. Conference: 12th Symposium of the Geological Society of Iran (In Persian with Enlish abstract).

[30]. Abbasnia, H., Karimpour, M.H., Malekzadeh Shafaroudi, A. (2019). Damanghor intermediate sulfidation epithermal Au mineralization, Northern Bardaskan: geology, alteration, mineralization, and geochemistry. Iranian Journal of Crystallography and Mineralogy. 27(3): 621-634 (In Persian with Enlish abstract).

[31]. Zuo, R. (2011). Identifying geochemical anomalies associated with Cu and Pb–Zn skarn mineralization using principal component analysis and spectrum–area fractal modeling in the Gangdese Belt, Tibet (China). Journal of Geochemical Exploration, 111, 13-22.

[32]. Farahmandfar, Z., Jafari, M.R., Afzal, P., Ashja Ardalan, A. (2020). Description of gold and copper anomalies using fractal and stepwise factor analysis according to stream sediments in NW Iran. Geopersia. 10 (1): 135-148.

[33]. Muller J., Kylander, M., Martinez-Cortizas, A., Wüst, R.A.J., Weiss, D., Blake, K., Coles, B., Garcia-Sanchez, R. (2008). The use of principle component analyses in characterizing trace and major elemental distribution in a 55 kyr peat deposit in tropical Australia: implications to paleoclimate. Journal of Geochemistry Cosmochemistry Acta 72, 449-463.

[34]. Hajnajafi, Gh., Jafari Rad, A.R., Afzal, P., Sheikhzakariaei, S.J. (2021). Geological interpretation using multivariate K-means and robust factor analysis in Dezak area, SW Iran. Environmental Earth Sciences volume. 80 (1): 1-13.

[35]. Mandelbrot, B.B. (1983). The fractal geometry of nature. Freeman, San Fransisco.mineralized zones in the Zaghia iron ore deposit, Central Iran. Journal of Geochemical Exploration, 122: 9-19.

تعیین پتانسیل های طلازایی براساس نمونه های سنگی با استفاده از آنالیز فاکتوری مرحله‌ای و مدل فرکتالی در منطقه بردسکن (شمال خاوری ایران)

لی‌لی دانشور صائین*

گروه زمین شناسی، دانشگاه پیام نور، تهران، ایران

ارسال ۲۰۲۱/۰۸/۳۱، پذیرش ۲۰۲۱/۱۰/۱۶

* نویسنده مسئول مکاتبات: daneshvar.saein@gmail.com

چکیده:

هدف اصلی این نوشتار تعیین پتانسیل های طلازایی براساس نمونه های سنگی با استفاده از آنالیز فاکتوری مرحله¬ای و مدل فرکتالی عیار-تعداد در منطقه بردسکن (شمال خاوری ایران) می باشد. در این منطقه دو تیپ کانه زایی اپی ترمال و پراکنده برای طلا دیده می شود. آنالیز فاکتوری مرحله‌ای در چهار مرحله صورت پذیرفت که در سه مرحله نخست هدف حذف عناصر مزاحم بود. در مرحله چهارم بر روی عناصر مربوط به کانه زایی طلا شامل طلا، آرسنیک، مس، آهن، روی، کادمیوم، نقره، مولیبدن، بیسموت، گوگرد و لانتانیوم صوت پذیرفت. عناصر در نهایت در چهار فاکتور دسته بندی شدند که گروه اول شامل مولیبدن، آرسنیک و گوگرد و گروه سوم شامل طلا و نقره هدف نهایی برای مدلسازی فرکتالی در نظر گرفته شدند. مدلسازی فرکتالی روی امتیازات فاکتوری ایندو گروه صورت گرفت و حدود آستانه‌ای هر دو فاکتور جدا شدند. پتانسیلهای حاصله بر این اساس در شمال خاوری، شمال و جنوب خاوری منطقه تعیین شدند. این پتانسیل ها با آلتراسیون های اصلی بخصوص سیلیسی شدن، سریسیتی شدن و کلریتی شدن در تطابق است. همچنین در همسایگی با گسلها و مطابق با تقاطع گسلها نیز می باشند. اصلی ترین پتانسیل در شمال خاوری منطقه است که با رگه و رگچه های سیلیسی، نمونه های مجدد برداشت شده با عیارهای بیش از ۱۰۰ ppb و تقاطع گسلها هماهنگی دارند.

کلمات کلیدی: کانه زایی طلا، روش فرکتالی عیار-تعداد، آنالیز فاکتوری مرحله ای، نمونه های سنگی، بردسکن.